heritage

MDPI

Article

An Integrated Diagnostic Approach to Deepen the Understanding of Michele di Matteo's Wooden Panel *Coronation of the Virgin*

Valeria Comite [1,*], Chiara Andrea Lombardi [1,2], Andrea Bergomi [1], Alfonsina D'Amato [3], Mattia Borelli [1], Gianluca Carabelli [1], Valentina Verzoni [4], Mario Colella [5,6], Daniele Bolleri [1], Vittoria Guglielmi [1] and Paola Fermo [1]

1 Dipartimento di Chimica, Università degli Studi di Milano, Via Golgi 19, 20133 Milano, Italy; chiara.lombardi@unimi.it or chiaraandrea.lombardi@uniroma1.it (C.A.L.); andrea.bergomi@unimi.it (A.B.); mattia.borelli@unimi.it (M.B.); gianluca.carabelli@studenti.unimi.it (G.C.); daniele.bolleri@studenti.unimi.it (D.B.); vittoria.guglielmi@unimi.it (V.G.); paola.fermo@unimi.it (P.F.)
2 Dipartimento di Scienze dell'antichità, Sapienza Università di Roma, Piazzale A. Moro 5, 00185 Roma, Italy
3 Dipartimento di Scienze Farmaceutiche, Università degli Studi di Milano, Via Mangiagalli 25, 20133 Milano, Italy; alfonsina.damato@unimi.it
4 Scuola di Restauro Botticino-Valore Italia, Via E. Cosenz 54, 20158 Milano, Italy; verzonivalentina@gmail.com
5 Dipartimento degli Studi Umanistici, Piazza del Lino 2, 27100 Pavia, Italy; mario.colella@unipv.it
6 Centro Studio e Conservazione Piccolo Chiostro, Via Riviera 20/22, 27100 Pavia, Italy
* Correspondence: valeria.comite@unimi.it

Abstract

This study presents a non-invasive, integrated and multidisciplinary diagnostic approach applied to the analysis of the altarpiece *Coronation of the Virgin*, attributed to Michele di Matteo (15th century). The investigation focused on the evaluation of a restoration intervention carried out in 2023 using quantitative colorimetric measurements to assess chromatic variations induced by surface treatments. Other non-invasive techniques, including multispectral imaging, hyperspectral imaging, Raman spectroscopy, and visible reflectance spectroscopy, were employed to investigate the painted surface, examine underlying features, and support the characterization and spatial distribution of pictorial materials through comparison with reference standards. Finally, the proteinaceous binding media used by the artist were investigated using nano-liquid chromatography coupled with tandem mass spectrometry (nLC-MS/MS), a sensitive, high-resolution analytical approach in the field of cultural heritage studies. Overall, the integrated approach documented chromatic changes induced by cleaning, revealed the preparatory drawing and previously unknown decorative elements by infrared reflectography, and confirmed the presence of pigments previously identified in earlier studies, allowing, in some cases, for an investigation of their distribution across the painted surface. The characterization of proteinaceous binding media further contributed to a deeper understanding of the materials and techniques employed by the artist.

Keywords: non-invasive analysis; restoration monitoring; colorimetric analysis; proteomic analysis of binders

Academic Editor: Marc Vermeulen

Received: 30 December 2025
Revised: 5 February 2026
Accepted: 13 February 2026
Published: 19 February 2026

1. Introduction

Scientific research applied to cultural heritage has become an essential tool for understanding historical artworks, evaluating their conservation conditions, and supporting

informed and sustainable restoration strategies. Over the past few decades, diagnostic methodologies have significantly evolved, with a growing emphasis on non-invasive approaches that allow for detailed material characterization without compromising the physical integrity of the artwork [1–7].

In the study of painted artworks, non-invasive analytical techniques are increasingly employed to support conservation processes alongside material investigations. Among these, visible reflectance colorimetry enables the objective documentation of chromatic variations and is particularly effective for monitoring cleaning treatments through measurements performed before and after restoration interventions [8–10]. Moreover, numerous studies have demonstrated the effectiveness of the integrated use of spectroscopic and imaging techniques, such as the combined use of multispectral imaging (MSI), hyperspectral imaging (HSI), and Raman spectroscopy [1,2,11–13].

Indeed, these analytical methods represent some of the most powerful non-invasive diagnostic tools currently available in the study of cultural heritage. When combined with other non-invasive and micro-invasive analytical techniques, they can produce integrated datasets that are highly valuable for technical art historical studies, condition assessments, and the planning of conservation interventions [14–16]. Such methodologies are increasingly applied in case studies aimed at improving the understanding of historical artworks and their conservation. In this context, a multi-technique diagnostic strategy primarily based on non-invasive imaging and spectroscopic methods was applied.

This integrated diagnostic approach was employed to study the altarpiece *Coronation of the Virgin*, attributed to Michele di Matteo, an artist active in Bologna during the early fifteenth century The present research builds on a previous study [17], which provided a preliminary analytical characterization of the artwork through a combination of techniques, including X-ray fluorescence (XRF), infrared reflectography (IRR) and X-radiography, scanning electron microscopy coupled with energy-dispersive X-ray spectroscopy (SEM-EDX), external reflection Fourier transform infrared spectroscopy (ED-FTIR), and optical microscopy. In the current work, the results of colorimetric measurements, MSI, HSI, visible reflectance spectroscopy, and Raman spectroscopy applied to the altarpiece are presented, thereby complementing the analytical strategy adopted in the earlier investigation and ultimately offering a more comprehensive characterization of the painting.

Colorimetric measurements were employed to assess the impact of a cleaning process applied to the altarpiece, whereas combined information from all other non-invasive techniques was used to obtain information on the painted surface and the underlying layers, as well as on the artist's painting technique and chromatic palette.

This study aims to deepen and expand current knowledge of the pictorial technique of Michele di Matteo, an artist of major historical and artistic relevance who has so far received limited scientific attention. The investigated altarpiece therefore represents a significant case study for the construction of a reference analytical dataset on the artist's pictorial production. The application of diagnostic techniques that are different from and complementary to those employed in the previous study allowed the integration and refinement of existing information, particularly with regard to the distribution of the main pigments and to observable material features of the painted surface. Moreover, the execution of investigations before and after the restoration, with particular emphasis on colorimetric measurements, provides reference values of the pictorial surface in post-treatment conditions. These data may serve as a baseline for future monitoring of potential degradation phenomena and to support more informed conservation decisions, also in relation to the exhibition or relocation context of the artwork. This approach may also represent a useful and potentially transferable tool for conservators in the study and preservation of comparable works.

Moreover, compared to traditional analytical protocols, a more sensitive and accurate analytical approach was adopted to study the binding media [18]. Classic approaches include gas chromatography coupled with mass spectrometry (GC-MS), a well-established technique for identifying natural organic binders such as drying oils and proteinaceous materials [19–23]. In this study, nano-liquid chromatography coupled with tandem mass spectrometry (nLC-MS/MS) was used in combination with bioinformatic approaches, optimized for the detection and sequencing of and proteins [18].

The integration of results from two diagnostic campaigns, conducted before and after the restoration, allows additional insights into the materials and technical aspects of Michele di Matteo's painting, within a broader multi-method analytical framework.

2. Materials and Methods

2.1. The Coronation of the Virgin Panel Painting

The *Coronation of the Virgin* (Figure 1) is one of the earliest and most representative artworks by Michele di Matteo da Bologna (active 1410–1469) [24]. It is likely the original central panel of a polyptych commissioned by the Corporazione dei Calzolari, of which the side panels are now lost [24]. The depicted scene shows the Virgin being crowned by Christ, seated on a richly decorated throne against a gilded background. The style, elongated figures, angular drapery, and gothic motifs, reflect the influence of Giovanni da Modena and the Bolognese devotional tradition. Instead, the partial inscription ("Matei F") may be a later autograph.

Figure 1. Michele di Matteo, *Coronation of the Virgin* (ca. 1410–1426), wooden panel, 98 × 71 cm. Visible light image of the artwork after the 2023 restoration intervention.

Scholars date the work between 1410 and 1426, and it is considered Michele di Matteo's earliest public commission [25,26]. Also known as Matteo de Calcina or Michele della Fornace, he was mainly active in Bologna and other northern Italian cities, producing altarpieces, frescoes, and stained-glass cartoons. Now part of the Ricasoli Collection in

Florence, the painting was restored in 2023 by the Centro Studi e Conservazione del Piccolo Chiostro, under the supervision of the Florence Superintendency.

2.2. Instrumental Techniques

The multi-analytical approach adopted in this study was carried out in two separate analytical phases, using non-invasive and minimally invasive techniques. In the first phase, the restoration was monitored by performing visible reflectance colorimetry before and after the cleaning phase, to evaluate chromatic changes and assess the effectiveness of the treatment. Instead, the second phase was conducted to investigate the presence of possible underdrawings and pentimenti, as well as to identify and map the artist's original paint palette and any previous retouching. In addition to colorimetric measurements, this phase involved the use of other non-invasive techniques such as MSI, HSI, visible reflectance spectroscopy, and Raman spectroscopy, supported by reference standards for data interpretation.

Finally, a preliminary proteomic investigation was carried out using nano-liquid chromatography coupled with tandem mass spectrometry (nLC-MS/MS) to perform an initial identification of proteins and gain insight into the possible paint binders used.

2.2.1. Visible Reflectance Colorimetry and Spectroscopy

A Konica Minolta CM-2300d portable spectrocolorimeter (manufactured by Konica Minolta, Inc., Tokyo, Japan) was used to study the surface of the altarpiece. For colorimetric measurements the instrument was operated in SCI (Specular Component Included) mode, whereas for spectroscopic measurements the spectral reflectance was measured between 360 and 740 nm, with a resolution of 10 nm. A measurement aperture of 8 mm in diameter was used, and data processing was carried out using the SpectraMagic NX (version 3.0) software. All measurements were performed directly on specific sites of the painting's surface before and after the cleaning treatment. Positioning, acquisition geometry and illumination conditions were reproduced with the highest possible accuracy. The CIELAB color space was adopted because it is perceptually uniform and designed to approximate human visual perception, making it particularly suitable for the assessment of chromatic variations in conservation studies. Color variations were quantified using the ΔE parameter, calculated using Equation (1):

$$\Delta E = \sqrt{\left(\Delta L^{*2} + \Delta a^{*2} + \Delta b^{*2}\right.} \quad (1)$$

Reflectance calibration of the system was performed using a two-point calibration procedure, employing the manufacturer-supplied white reference standard as the 100% reflectance reference and a measurement in air, in the absence of reflective surfaces within the field of view, as the 0% reflectance reference.

2.2.2. Multispectral Imaging

The MSI system (MADAtec S.r.L.) employed in this study is based on a modified Samsung NX3300 mirrorless camera (manufactured by Samsung Electronics Co., Ltd., Suwon, Republic of Korea) converted to "full spectrum" by removing the internal UV/IR-cut filter, thereby extending the sensitivity of the CMOS APS-C 20.3 MP (manufactured by Samsung Electronics Co., Ltd., Suwon, Republic of Korea) sensor to a broad spectral range (300–1100 nm). An Auto Beroflex MC 28 (manufactured by Beroflex Kamera-Film Aktiengesellschaft, Berlin/Bad Kissingen, Germany) mm f/2.8 lens (76° field of view, 52 mm diameter) was coupled via a Kecay PK-NX (manufactured by Kecay/Shenzhen Longgang District factory, Shenzhen, China) mount adapter. To ensure proper chromatic

balance during image acquisition, a reference standard made of calcium sulfate dihydrate ($CaSO_4 \cdot 2H_2O$) was used as a neutral target.

Table 1 summarizes the acquisition settings, including optical filters and illumination sources employed for the different MSI modalities.

Table 1. Multispectral imaging techniques used for pigment identification on the analyzed painting.

Imaging Technique	Acronym	Filter	Light Source
Visible Spectrum	Vis	UV&IR Cut (band-pass 390–700 nm)	Sunlight, fluorescent lamp or tungsten filament lamp
Near-Infrared Reflectography	IRR720 IRR850 IRR950	IR720 (high-pass > 720 nm) IR850 (high-pass > 850 nm) IR950 (high-pass > 950 nm)	100 W tungsten filament lamp
UV-induced Visible Luminescence	UVL Vis	UV&IR Cut (band-pass 390–700 nm)	UV LED lamp 365 nm
UV-induced Infrared Luminescence	UVL IR720 UVL IR850 UVL IR950	IR720 (high-pass > 720 nm) IR850 (high-pass > 850 nm) IR950 (high-pass > 950 nm)	UV LED lamp 365 nm
Visible-induced Visible Luminescence	VIVL	Yellow filter HP500 (high-pass > 500 nm)	Blue LED torch 440 nm

False-color images (IRFC) were generated in post-processing by combining an IRR image and a visible photograph taken from the same viewpoint. The final RGB image was reconstructed by assigning the infrared channel to red (R), and two visible components to green (G) and blue (B), depending on the selected false-color mode (IRGB or IRRG). Image processing was performed using RawTherapee (version 5.8, for white balance and exposure adjustments), Adobe Photoshop (version 2023/2024, for precise image alignment), and ImageJ (version 1.54, for RGB channel recomposition). False-color imaging was employed to assist in pigment identification, reveal chromatic overlaps, and detect underdrawings or non-original interventions.

2.2.3. Hyperspectral Imaging

HSI was carried out using a Specim IQ portable hyperspectral camera (manufactured by Specim, Spectral Imaging Ltd., Oulu, Finland; a Konica Minolta company, model 0604675), equipped with a push-broom CMOS sensor (512 × 512 pixels, manufactured by Sony Semiconductor Solutions, Tokyo, Japan), in the 400–1000 nm spectral range, with a spectral resolution of 7 nm. The system was mounted on a tripod and operated with integration times ranging from 1 to 500 ms. The artwork was irradiated using natural sunlight, which served as the illumination source for the acquisition of the hyperspectral data cubes. The use of this radiation allowed adequate coverage of the entire spectral range of the camera and enabled the collection of data suitable for subsequent processing.

All hyperspectral acquisitions were performed in an outdoor environment. To account for possible variations in solar illumination, a reflectance normalization procedure was applied using the calibrated white reference standard supplied with the system, consisting of a diffusive material with high reflectance in the VIS–NIR spectral range. The reference standard was placed within the field of view and acquired simultaneously with the artwork. Dark current correction was performed by acquisition with the shutter closed, following the standard operating procedures of the Specim IQ system. Acquisitions were conducted under stable illumination conditions to minimize variations in solar radiation during data collection. The total acquisition time for each hyperspectral cube was on the order of a few minutes, while the integration time for each pixel spectrum did not exceed 99 ms.

The Specim INSIGHT software (version 1.4) [27] was used to process HSI data, including area extraction and averaging. The program also allowed the import and management of hyperspectral data cubes and supported spectral comparison procedures with reference curves. The spectra considered for the analysis were in the range of 400–740 nm. In particular, spectral curves acquired from the reference standards (pigment charts) were compared with those recorded on the painting. For each region, the average reflectance curve of the pixels belonging to the ROI was calculated, providing a representative spectral signature of the area.

2.2.4. Micro-Raman Spectroscopy

Raman measurements were conducted with a portable modular spectrophotometer (manufactured by B&W Tek LLC, Plainsboro, NJ, USA) equipped with a microscope and an in situ spectra acquisition system. A 785 nm excitation laser (manufactured by Thorlabs Inc., Newton, NJ, USA) was used with a nominal power of 450 mW. Signal attenuations from the fiber and probe resulted in less power reaching the sample (1–5% of the nominal power). The instrument was equipped with a silicon detector. The working range was selected between 56 and 3350 cm^{-1}. Finally, the probe (d = 9.42 mm) was operated at a working distance of 5.5 mm, resulting in an 85 µm diameter of the laser spot in the focal plane. Raman spectra were acquired using an integration time of 5000 ms and a spectral resolution below 5 cm^{-1}. Only dark subtraction was applied prior to spectral interpretation. Species identification was obtained by comparing the spectra recorded on the frescoes with those reported in the literature [28].

2.2.5. Nano-Liquid Chromatography Coupled with Tandem Mass Spectrometry

Micro pieces of different samples were collected during the restoration on the borders of the painting, without any damaging of the artwork. The whole protein was extracted by using a buffer composed of 8 M urea in 50 mM Tris-HCl, 30 mM NaCl at 8.5 pH (Sigma-Aldrich Co., St. Louis, MO, USA), followed by centrifugation at 14,000× *g* and 4° C for 10 min. Then, the extracted proteins were diluted in 50 mM NH_4HCO_3, reduced with 5 mM DL-dithiothreitol for 30 min at 52 °C, and then centrifuged at 500 rpm and alkylated with 15 mM iodoacetamide for 20 min in the dark at room temperature. The trypsin digestion was performed at a 1:20 enzyme/protein ratio (*w*/*w*) overnight at 37 °C. The analysis was performed using a Dionex Ultimate 3000 nano-LC system connected to an Orbitrap Fusion™ Tribrid™ Mass Spectrometer equipped with a nano-electrospray ion source (manufactured by Thermo Fisher Scientific Inc., Waltham, MA, USA). Tryptic peptides were separated on an EASY-Spray 50 cm × 75 µm ID column packed with Thermo Scientific Acclaim PepMap RSLC C18 column (3 µm, 100 Å particles). The flow rate was 300 nL/min, and the temperature was set to 35 °C. Each sample was analyzed in three technical replicates. A blank sample was injected after each triplicate to avoid sample carryover.

The raw files were processed using the MaxQuant proteomics software package (version V1.6.6.0), including the Perseus software platform (version 1.6.2.1, Max-Planck-Gesellschaft, München, Germany). The MS/MS spectra (raw files) were searched against a merged protein sequence database consisting of a Mammals proteome database (8,061,593 reviewed sequences) and Gallus Gallus proteome database (78,934 reviewed sequences). The settings used included fixed modifications for carbamidomethyl (C), and variable modifications for oxidized methionine (M) and acetyl (N-terminus). High-confidence and unique peptides (minimum 1 peptide per protein at a PSM FDR of 0.01 and protein FDR of 0.01) were used for protein identification [29].

Blast analyses were performed using the Uniprot application, targeting homolog sequences across different species by querying the accession numbers of the identified proteins.

2.3. Reference Standard Pigments

A set of reference standards was employed to validate the results obtained with non-invasive analytical techniques. For this purpose, standardized color charts provided by Kremer Pigmente GmbH were used [30]. These consist of paper samples coated with pure pigments, each identified by unique codes, commercial names, and, where available, detailed information on their composition, particle size, and provenance. The pigment standards were analyzed under the same acquisition conditions applied to the painting, ensuring spectral and chromatic comparability. The identification procedure relies on a direct comparison between unknown and known pigments, based on the similarity.

3. Results and Discussion

3.1. Monitoring of the Cleaning Restoration Process

To evaluate the impacts of the cleaning procedure, the analyses were carried out in two separate measurement campaigns, before and after the restoration treatment. Given the visually observed fragile condition of the paint layer and the evidence of previous invasive cleaning, the intervention was limited to the careful removal of superficial dirt deposits. Under these conditions, no specific chromatic change was expected a priori; rather, colorimetric analyses were used to objectively document the chromatic variations between the pre- and post-cleaning states and to support conservation decisions regarding the extent of the cleaning and the appropriateness of not proceeding further with more invasive treatments. Figure 2 shows the location of 29 representative measurement points on the panel, selected from a larger set of acquisitions upon the restorer's recommendation.

The results were processed using the CIELAB system (SCI mode), and ΔE values were calculated to assess overall perceptible differences (Table 2). In general, a widespread increase in the L* parameter following the cleaning treatment was observed, indicating enhanced brightness of the painted surface, consistent with the removal of surface dirt, or oxidized patinas. Instead, variations in a* and b* parameters were more localized. In many cases, changes in chromatic coordinates were moderate, suggesting that the cleaning process primarily affected surface brightness rather than significantly altering hue or saturation. Based on these results, the outcome of the cleaning was considered satisfactory from a conservation point of view, and the colorimetric assessment supported the decision not to proceed further with more invasive cleaning operations.

Notable chromatic shifts were recorded only on the cushion and the Virgin's mantle, specifically at the red measurement points located on these areas (Figure 2). In the first case, a marked increase in a ($\Delta a = +10.62$) was observed, consistent with a more saturated red. This behavior is corroborated by the high ΔE values measured in the red areas of the cushion (>13 at points 3.R and 4.R), indicating clear chromatic changes. These results are due to the impact of the restoration, in which the restorers applied a red cadmium-based pigment to certain areas of the cushion where small superficial losses of the original red paint layer were detected. The removal of an oxidized varnish also revealed a color shift from green to blue ($\Delta b^* = -6.19$), as measured at point 7B.

Finally, ΔE values greater than 5 were primarily found in the lighter areas of the composition, such as flesh tones, architectural elements, and the base of the throne. In these areas, the increase in L* values suggests that the treatment brought the painting closer in appearance to its original state. In this perspective, the colorimetric values recorded after

cleaning may be considered a useful baseline reference for future monitoring activities aimed at assessing possible surface re-soiling over time.

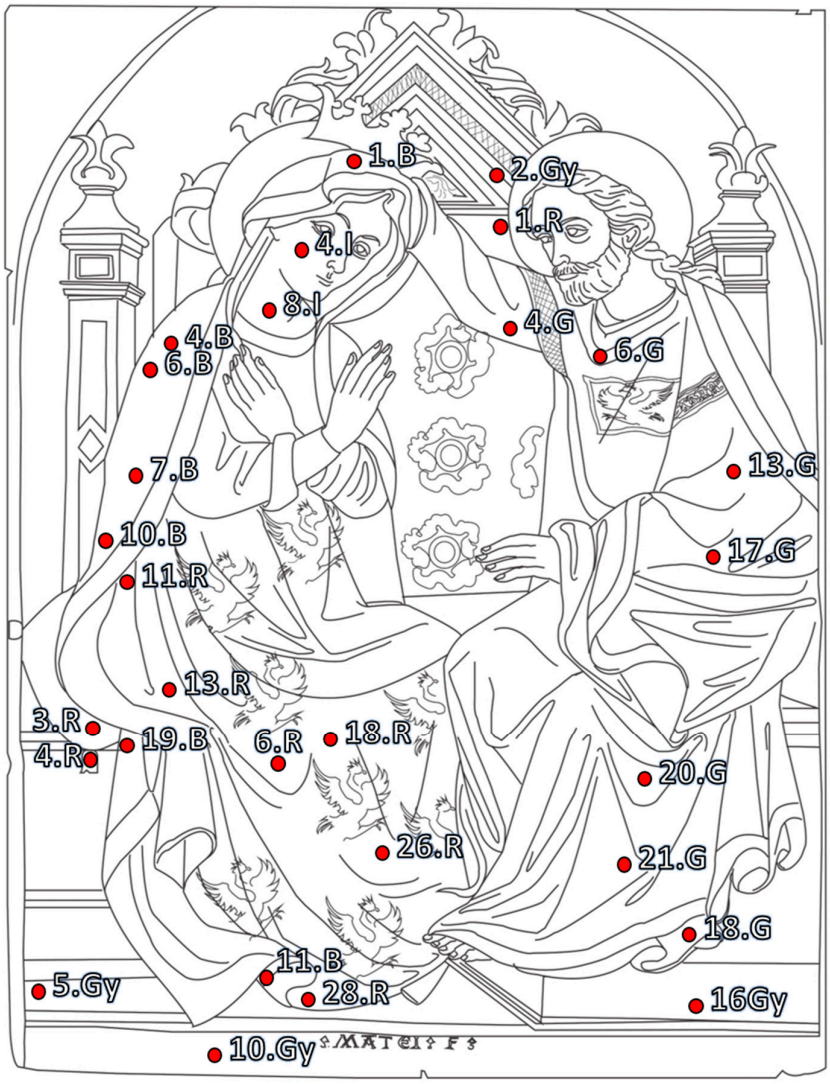

Figure 2. Image of the panel showing the 29 points selected for colorimetric measurements before and after the restoration treatment. The letters indicate the colors: R = red, B = blue, G = green, Gy = grey, I = incarnate.

Table 2. CIELAB colorimetric data (SCI mode) for 29 representative points on the painting, comparing pre- and post-restoration measurements. The letters indicate the colors: R = red, B = blue, G = green, Gy = grey, I = incarnate.

Point	Before/After Restoration	L*(D65)	a*(D65)	b*(D65)	ΔL	Δa	Δb	ΔE
1.B	Before	30.42	0.01	1.42	−2.68	−1.09	−1.44	3.23
1.B	After	27.74	−1.08	−0.02				
4.B	Before	31.07	−2.35	0.01	0.13	−1.73	−3.30	3.72
4.B	After	31.20	−4.08	−3.29				
6.B	Before	30.46	−0.69	1.12	−1.75	−2.13	−4.29	5.10
6.B	After	28.71	−2.82	−3.17				
7.B	Before	30.76	−0.56	2.00	−4.86	−1.80	−6.19	8.07
7.B	After	25.90	−2.36	−4.19				

Table 2. *Cont.*

Point	Before/After Restoration	L*(D65)	a*(D65)	b*(D65)	ΔL	Δa	Δb	ΔE
10.B	Before	30.20	−0.03	2.03	−3.42	−1.64	−3.89	5.43
10.B	After	26.78	−1.67	−1.86				
11.B	Before	32.47	0.02	3.94	1.15	−5.50	−5.15	7.62
11.B	After	33.62	−5.48	−1.21				
19.B	Before	33.24	−2.45	0.42	−1.29	−1.94	−3.07	3.85
19.B	After	31.95	−4.39	−2.65				
4.I	Before	40.27	13.12	16.28	9.71	1.97	0.26	9.91
4.I.	After	49.98	15.09	16.54				
8.I	Before	53.40	10.73	23.55	3.61	−1.39	−2.24	4.47
8.I	After	57.01	9.34	21.31				
1.R	Before	31.60	10.40	7.64	2.31	4.60	3.80	6.40
1.R	After	33.91	15.00	11.44				
3.R	Before	33.30	18.71	12.15	6.12	10.62	6.31	13.79
3.R	After	39.42	29.33	18.46				
4.R	Before	34.69	16.23	12.54	5.55	10.47	7.03	13.78
4.R	After	40.24	26.70	19.57				
6.R	Before	31.02	14.16	7.46	0.94	4.36	1.68	4.77
6.R	After	31.96	18.52	9.14				
11.R	Before	31.33	11.17	6.91	2.82	3.74	4.66	6.61
11.R	After	34.15	14.91	11.57				
13.R	Before	34.63	17.24	12.33	1.02	2.70	1.21	3.13
13.R	After	35.65	19.94	13.54				
18.R	Before	40.34	10.75	13.94	−0.93	7.46	1.20	7.61
18.R	After	39.41	18.21	15.14				
26.R	Before	29.21	9.79	5.77	1.14	3.01	2.12	3.85
26.R	After	30.35	12.80	7.89				
28.R	Before	36.65	15.62	10.71	1.03	1.76	0.18	2.05
28.R	After	37.68	17.38	10.89				
4.G	Before	29.46	1.24	2.94	−1.51	−1.18	−0.16	1.92
4.G	After	27.95	0.06	2.78				
6.G	Before	31.21	−0.47	2.93	−2.52	−2.81	−2.42	4.48
6.G	After	28.69	−3.28	0.51				
13.G	Before	28.15	0.48	1.84	−0.90	−1.00	0.14	1.35
13.G	After	27.25	−0.52	1.98				
17.G	Before	28.12	0.67	1.97	−0.93	−0.54	0.41	1.15
17.G	After	27.19	0.13	2.38				
18.G	Before	29.74	0.30	6.79	1.60	−0.96	−0.75	2.01
18.G	After	31.34	−0.66	6.04				
20.G	Before	28.99	3.23	3.11	−1.09	−0.57	−0.32	1.27
20.G	After	27.90	2.66	2.79				
21.G	Before	30.76	3.65	4.92	0.41	1.09	1.53	1.92
21.G	After	31.17	4.74	6.45				
2.Gy	Before	40.83	7.02	14.62	13.28	0.45	−1.29	13.35
2.Gy	After	54.11	7.47	13.33				
5.Gy	Before	43.40	6.93	21.61	18.59	−1.38	0.06	18.64
5.Gy	After	61.99	5.55	21.67				
10.Gy	Before	38.52	6.90	16.97	1.58	−0.50	−0.83	1.85
10.Gy	After	40.10	6.40	16.14				
16.Gy	Before	48.51	5.17	20.62	12.80	−2.09	−1.31	13.03
16.Gy	After	61.31	3.08	19.31				

3.2. Underdrawings and Pentimenti

The preparatory layer of the painting was observed with IRR using the IRR950 filter (high-pass > 950 nm), highlighting several features of the artist's creative process. For instance, as shown in Figure 3, the facial features of the figures and the decorative details of the throne and of the Virgin's dress appear more visible in the infrared images. The drawing lines and brushstrokes were also more clearly highlighted, demonstrating a meticulous compositional plan by the artist.

Figure 3. Image of the artwork: acquisition in visible light (**a**) and in IRR950 in grayscale (**b**). Details: Virgin's face in visible (**c**) and IRR950 in grayscale (**d**); Christ's face in visible (**e**) and IRR950 in grayscale (**f**); Virgin's skirt and throne in visible (**g**) and IRR950 in grayscale (**h**); signature in visible (**i**) and IRR950 in grayscale (**l**).

IRR also revealed the use of punch decoration, a typical medieval painting technique used to embellish gilded surfaces. This method was often employed to create ornamental motifs on halos and on the decorative borders of sacred vestments. Overlapping punch marks are also evident on the Virgin's crown and halo, whereas Christ's halo shows signs of pigment layers applied on the gilded surface to render the hair.

Another detail that is not evidently observable in the visible images is Christ's crown. This observation suggests two possible interpretations: either a change of heart by the artist, whereby the crown, initially painted and decorated, was subsequently concealed; alternatively, it could indicate a loss of gilding caused by later restoration interventions or by material degradation. This kind of "revised" punching is documented in other Gothic panel paintings where artistic revisions were carried out after the punching using a brush [31]. In the painting, phytomorphic motifs in relief were also noted on the Virgin's dress and on the backrest of the throne, thanks to IRR observations.

Finally, on the lower edge of the panel (Figure 3), a deteriorated and barely legible inscription was discovered beneath the current signature "Matei F." The inscription observable under visible light was added later, perhaps to replace the original signature, which is not legible anymore [32].

3.3. Reconstruction of the Paint Palette

The results obtained from MSI, HSI, and visible reflectance colorimetry were compared to confirm the chromatic palette previously identified by Delledonne et al. (2024) [17] and evaluate possible additional features. All the investigations with imaging techniques were acquired on the restored painting after the most recent restoration performed in 2023 to avoid interferences from oxidized varnishes, altered patinas or surface dirt. The spectral data obtained were compared with standardized pigment color charts, recorded under the same operating conditions.

Figure 4a shows that red pigments are distributed in four different areas of the composition: the Virgin's robe, the cushion, the throne's backrest, and the phytomorphic decorations surrounding the throne. Regions that appear red in the visible images shift to yellow–orange in IRRG and remain red in IRGB observations. The same false-colour response is reproduced by the Kremer reference standards of cinnabar (HgS) and red ochre (Fe_2O_3); hence, unambiguous pigment identification was not possible.

Figure 4. Visible image (**a**); IRRG false-color image (**b**); IRGB false-color image (**c**) of the altarpiece.

In the previous study by Delledonne et al. (2024) [17], cinnabar was identified by XRF through the detection of Hg. Instead, red ochre was recognized by combining XRF results, which showed the presence of Fe, and ER-FTIR observations, which highlighted the presence of Fe–O and silicate bands. The occurrence of both red pigments in similar areas may reflect the use of a mixture of the two, with red ochre likely employed as a darkener to modulate tones and shadows.

The cadmium red Kremer standard also showed a similar false-color behavior. This is an industrial pigment introduced between the late nineteenth and early twentieth centuries and is therefore incompatible with the painting's chronology. Nonetheless, the reference standard was tested based on information from the restorers, who reported the use of cadmium-based pigments during overpaints on small areas of the cushion. Indeed, near-infrared fluorescence under UV excitation revealed localized retouching on this element of the painting, consistent with the behavior of cadmium red (Figure S1 in Supplementary Materials).

To identify the areas where the hypothesized pigments, or possible mixtures of them, could be present, the HSI data were analyzed to evaluate their spatial distribution, using reference standards to guide the interpretation. The normalized reflectance spectra of the

pigments were obtained from the average spectral curves of the pixels belonging to the corresponding mapped areas (Figure 5c).

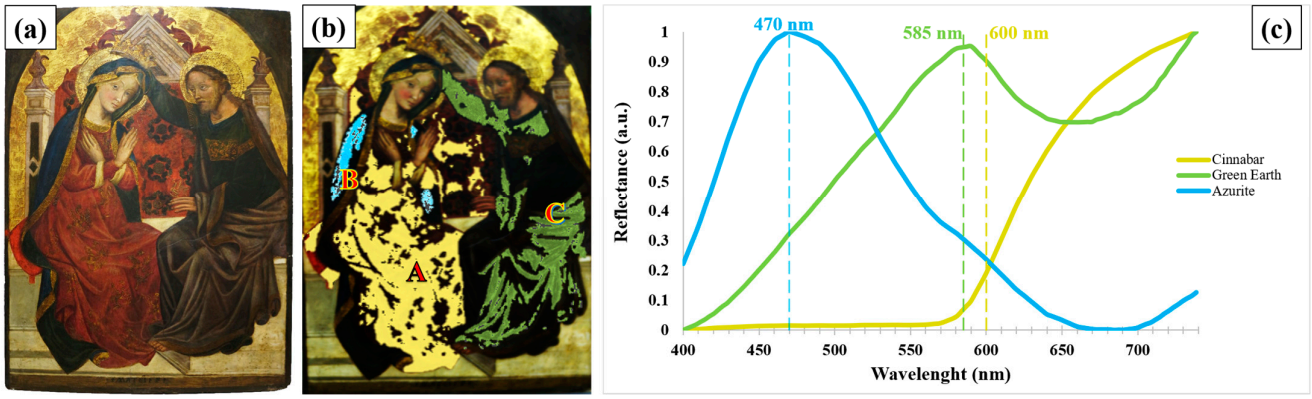

Figure 5. Visible image of the altarpiece (**a**) together with the distribution map highlighting the areas where each pigment was detected (**b**) and the reflectance spectra (**c**). **A** indicates areas rich in cinnabar, **B** areas attributed to azurite, and **C** areas attributed to green earth.

Starting from cinnabar, Figure 5b shows the distribution of this pigment across the painting, mainly in the Virgin's dress (area A), in parts of the throne's backrest, and in areas of the cushion. The visible reflectance spectrum reported in Figure 5c highlights the characteristic sigmoidal profile of this pigment, with low reflectance values in the blue–green region, a rapid increase in the red region, and high reflectance values approaching a plateau beyond 650 nm [33,34]. In the distribution map shown in Figure 5b, the areas attributed to cinnabar are highlighted in yellow. The remaining unclassified regions, which appear uncolored in the map, correspond to areas where the spectral response did not exhibit sufficiently diagnostic features to allow an unambiguous attribution. This is likely due to the presence of pigment mixtures, surface alterations, or overlapping contributions that make the spectral signature less recognizable within the visible range.

The presence of cinnabar was also confirmed by micro-Raman spectroscopy. Figure 6 highlights the characteristic peaks at 253, 289, and 343 cm^{-1}, in agreement with reference data [28,35].

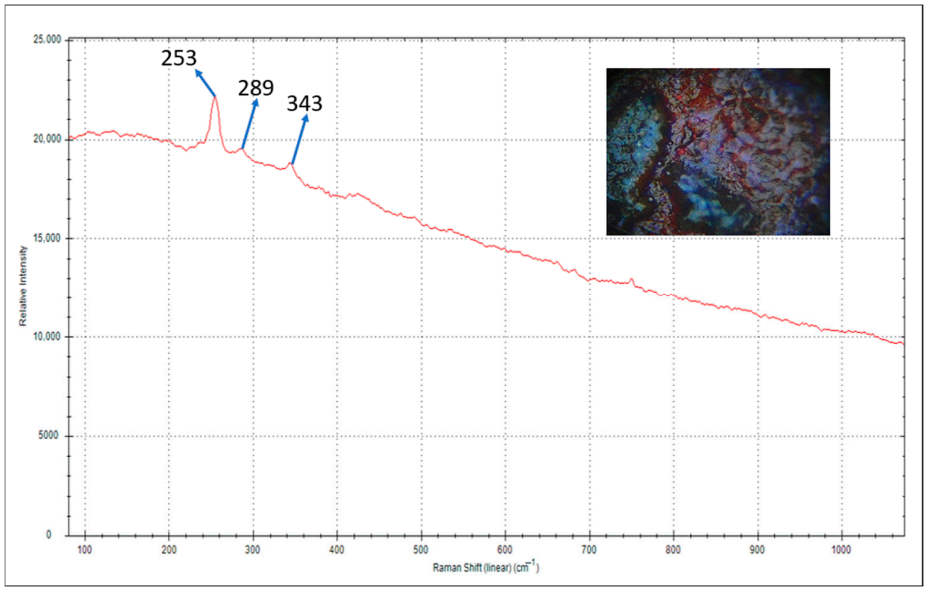

Figure 6. Raman spectrum acquired on a red area of the Virgin's robe, showing the characteristic peaks of cinnabar.

Other red areas of the painting could not be confidently identified by visible reflectance analysis and therefore remain unassigned. These areas may indicate the presence of an additional red pigment, plausibly red ochre, which is known to exhibit weakly diagnostic and often noisy reflectance spectra in the visible range. Moreover, practical factors such as support orientation and illumination conditions, together with microstructural aspects including pigment particle size and surface roughness, as well as compositional factors related to binders and varnishes, may further limit the reliable identification [33] and spatial mapping of these red areas.

Moving on to the blue pigments (area B), Figure 4 indicates that they are found predominantly in correspondence with the Virgin's mantle. In the study by Delle Donne et al. (2024) [17], azurite, Prussian blue and smalt were reported as possible blue pigments present in the painting. A comparison of the IRRG and IRGB images (Figure 4b,c) did not allow an unambiguous distinction among these materials due to the similarity of their responses in the infrared range.

In contrast, hyperspectral imaging supported the identification of azurite, while no diagnostic spectral features attributable to Prussian blue or smalt were observed. In the same study [17], azurite had already been proposed as part of the original palette on the basis of copper detected by XRF analysis. The azurite distribution mapped by HSI in the present study further confirms the presence of this pigment, showing areas located on the Virgin's mantle characterized by a light blue tonality (Figure 5b). The visible reflectance spectrum acquired from these areas (Figure 5c) displays features compatible with azurite, including a reflectance maximum around 470 nm and a slight depression near 650 nm, in agreement with literature data [35].

Moving on to the green pigments, these pigments were observed mainly on Christ's robe (Figure 4). The study by Delle Donne et al. (2024) [17] suggested the presence of green earth ($K(Al,Fe^{3+}),(Fe^{2+},Mg)O_{10}(OH)_2$) and malachite ($CuCO_3{\cdot}Cu(OH)_2$) based on XRF measurements showing signals consistent with those of Fe, Si, and Cu. Instead, analyses carried out in this technique only allowed the detection of the green earth pigment (area Ccadmium). Indeed, this pigment appears grey in the IRRG image and brown in the IRGB image (Figure 4). This behavior is likely related to the use of multiple and different pigments combined within the paint layers to achieve the final chromatic effect. The reflectance spectrum shows a broad maximum around 585 nm (Figure 5c), together with a slight shoulder, features that are characteristic of green earth pigments.

The shift in the reflectance maximum with respect to the value commonly reported in the literature (around 560 nm [36]) may be related to factors such as pigment granulometry, the nature of the binding medium, the thickness of the paint layer, as well as illumination conditions and image acquisition parameters [37,38]. Furthermore, it is well known that the absorption behavior of green earth results from an interaction between the two valency states of iron, where the Fe^{2+}/Fe^{3+} ratio correlates with variations in the pigment colour and, consequently, with shifts in the position of the reflectance maximum and shoulder [36,39]. In any case, the visible reflectance spectrum of green earth is diagnostic, as it clearly differs from those of brighter green pigments such as malachite and verdigris, which are characterized by sharper reflectance peaks shifted toward shorter wavelengths, typically in the range 490–520 nm [39,40]

Visible reflectance spectroscopy was then carried out to confirm the main pigments used in the execution of the painting, previously hypothesized through MSI and HSI. The analyses focused on specific sites in the red areas (Virgin's robe and throne), blue areas (Virgin's mantle), and green areas (inner robe of the Virgin and Christ's garment).

A total of 18 representative site-specific points were selected on the painted surface (Figure 7).

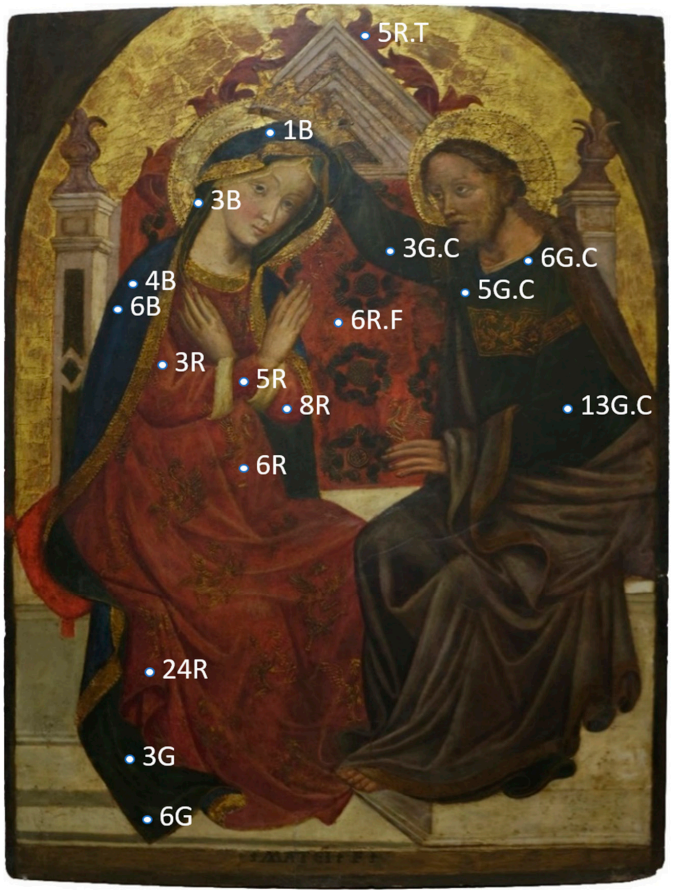

Figure 7. Location of the points investigated by visible reflectance spectroscopy. Letters R, B, and G indicate the dominant color at the spot (R = red, B = blue, G = green), while letters F, T, and C specify the corresponding pictorial element (F = flowers, T = throne, C = Christ).

The presence of the pigments was confirmed by comparing the normalized reflectance spectra and the first derivative to standard references, all acquired under the same conditions. For clarity and conciseness, only one representative spectrum is shown for each color group, as all measurement points within the same chromatic area exhibited consistent and reproducible spectral responses. Analyses of points 3R, 5R, 6R, 24R, 5R.T and 6R.F (Figure 8a,b) confirmed the use of red ochre. This is evidenced by the characteristic spectra, showing an increase around 500 nm and a shoulder around 675 nm [34,41].

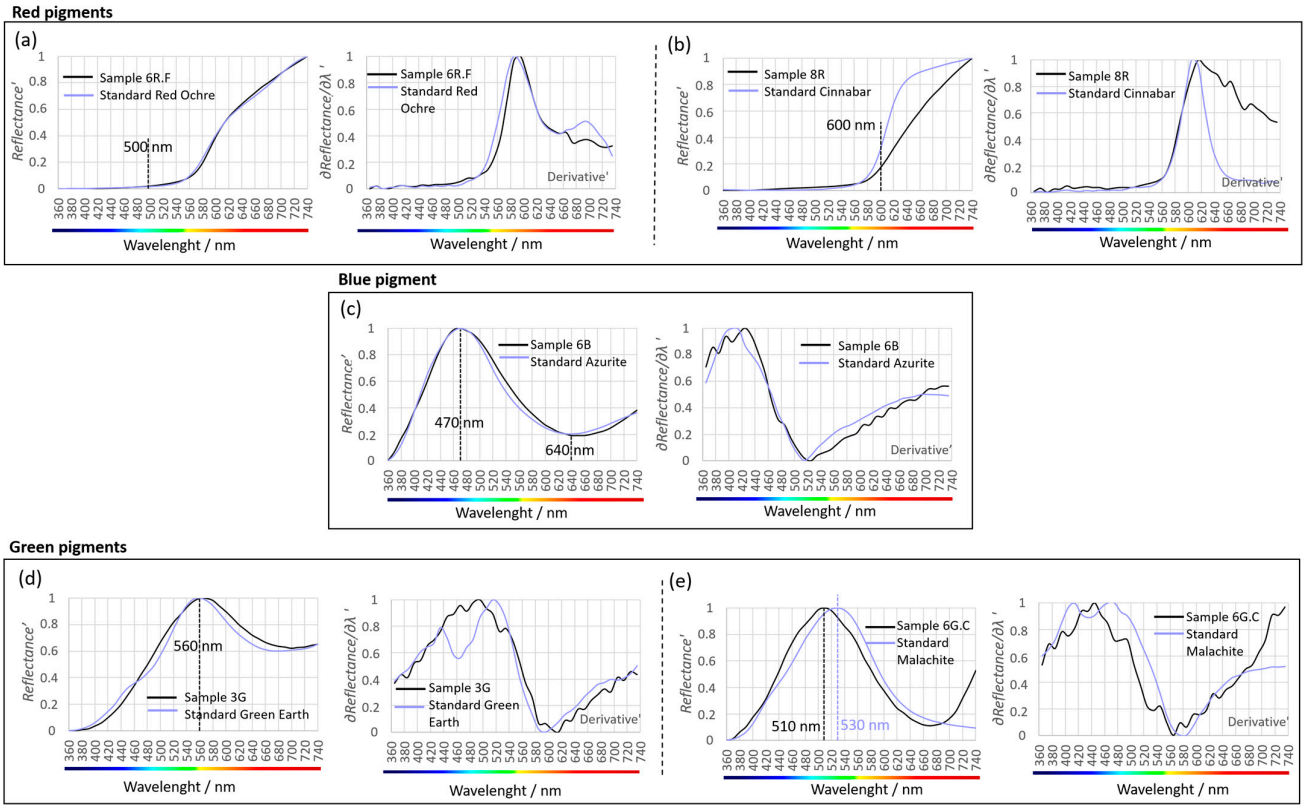

Figure 8. Visible Reflectance Spectra. Comparison between the spectra acquired from selected points on the artwork and those of standard pigments from Kremer Pigment. Each graph presents the normalized reflectance profile and its first derivative, used to confirm the identification of the main red (**a**,**b**), blue (**c**), and green pigments (**d**,**e**).

HSI observations presented earlier indicated the presence of cinnabar in some of the same areas in which red ochre was detected, suggesting their use as mixtures to create more nuanced shades and complex chromatic transitions. In fact, the reflectance spectra of points 6R and 8R (Figure 8a,b) display the general shape of a red ochre with an enhanced sigmoidal inflection shifted toward 600 nm, indicative of a possible mixture with cinnabar [42].

With regard to the blue pigments, the reflectance spectra of points 1B, 4B, and 6B (Figure 8c) located on the Virgin's mantle exhibit a maximum between 480–500 nm and strong absorbance around 640 nm, as typically seen for azurite [35,43]. This result further supports the attribution of this pigment.

Finally, the green pigment used on the Virgin's inner robe and Christ's garment was identified as green earth, based on the spectral signatures from points 3G, 6G, 3B, 3G.C, 5G.C, and 13G.C (Figure 8d), as was suggested by the imaging techniques. The spectra showed the characteristic reflectance maximum around 560 nm, consistent with literature data [36].

A darker bluish-green pigment was instead detected by visible reflectance analysis specifically on the collar of Christ's robe (point 6G.C, Figure 8e). The spectral profile of this localized area closely resembles that of malachite, while also showing partial overlap with verdigris. Since the identification is not based on the reflectance maximum alone, this material is more appropriately referred to as a copper green (malachite/verdigris or a possible mixture), and a definitive distinction between these pigments cannot be achieved by VIS reflectance alone.

Importantly, the copper-green features observed on Christ's collar do not rule out the possibility that this pigment results from a localized alteration of azurite [44,45]. Such alteration may be limited and superficial, generating greenish-bluish hues visible to the naked

eye but difficult to resolve through hyperspectral imaging because of spectral averaging and optical mixing. This localized degradation process could therefore account for the copper-green signatures detected in the VIS reflectance data but not clearly distinguished in the hyperspectral results, without undermining the attribution of green earth in the other areas of Christ's garment.

The main pigments identified in the painting and the diagnostic features used for their attribution are summarized in Table 3.

Table 3. Summary of pigment identification and diagnostic features.

Pigment/Material	Technique(s)	Diagnostic Features Used
Cinnabar (HgS)	MSI, HSI, reflectance spectra, Raman	MSI: red → yellow–orange in IRRG and red in IRGB; reflectance spectra: sigmoidal profile with low reflectance in the blue–green region, rapid increase in the red region and plateau beyond 650 nm; Raman: peaks at 253, 289, 343 cm^{-1}
Red ochre (Fe_2O_3)	reflectance spectra	Reflectance spectra: increase around ~500 nm with a shoulder near ~675 nm
Cadmium red (modern retouching)	UV-induced luminescence	Localized fluorescence response under UV excitation compatible with cadmium red
Azurite	HSI, reflectance spectra	Reflectance spectra: maximum around ~480–500 nm and strong absorption around ~640 nm
Green earth	MSI, HSI, reflectance spectra	MSI: grey in IRRG and brown in IRGB images; reflectance spectra: broad maximum around ~560–585 nm with a slight shoulder
Copper green (malachite/verdigris or mixture)	Reflectance spectra	Reflectance spectra: sharper maxima shifted toward ~490–520 nm, partially overlapping between malachite and verdigris

3.4. Protein Identifications of Paint Binder

The proteomic workflow employed combines nano-liquid chromatography with high-resolution tandem mass spectrometry (nLC-MS/MS) and advanced bioinformatic analysis, enabling the identification of proteins present in trace amounts. This cutting-edge methodology results in the accurate characterization of protein components in microscopic residues that may have previously been discarded during restoration processes.

The microscopic residues, discarded during restoration processes, were extracted using a denaturing buffer that allowed the following endoprotease digestion to produce the peptide mixture. After C18 zip purification and concentration, the peptide mixture was analysed by nano-liquid chromatography and tandem high-resolution mass spectrometry. The retention time of peptides, the m/z value of peptides and their fragments and the internal amino-acid sequences were used to identify the proteins present in the samples by online software based on protein databases. The first search was against the "Mammals" Uniprot database containing all the mammal protein sequences. The main identified proteins were related to well-known paint ligands, potential contaminants and aggregated proteins to binders [46]. Several isoforms of mammal collagens, two were *Bos taurus* (G1PR85, G1PSJ6), one from *Oryctolagus cunicilus* (G1T4A5), one from *Cavia porcellus* (H0VHD0) and one from *Gallus Gallus* (A0A8V1A970), the main components of animal glue, were identified by 15 sequenced peptides (Table 3). Beta casein (P02666), another known ligand, was identified by one peptide of sequence: DMPIQAFLLYQEPVLGPVR. Albumin

was characterized by two peptides, FQNALLVR and KVPQVSTPTLVEVSR (Table 3). Blast analyses were performed using the accession numbers of the identified proteins, to describe the homolog proteins. The analysis assesses the homology between protein sequences across different species. This approach ensures the reproducibility and allows for precise cross-species comparisons based on identified accession numbers. High sequence homology suggests a similar likelihood of these proteins being present in the sample (Table 3). For example, the Beta Casein (P02666) shows 100% homolog to *Bos taurus*, *Bos mutus*, *Bison bison*, *Bos indicus* and *Bos mutus* Grunnies. In contrast, other entries, identified by Blast, exhibit lower homology levels, below 70%.

To confirm the presence of ovalbumin from chicken, the raw data were assessed against the Uniprot "*Gallus-Gallus*" protein database (Table 4 and Supplementary Materials Table S1).

Table 4. Identified proteins in the samples from the wooden panel; identification has been carried out by Mammals and Gallus Gallus protein databases [29].

Protein Name	Accession Number	Peptide Sequence	MW(Da)	N Peptides	Taxonomy
Beta-casein	P02666	DMPIQAFLLYQEPVLGPVR	23,583	1	*Bos taurus*, *Bos taurus*, *Bos mutus*, *Bison bison*, *Bos indicus* and *Bos mutus Grunnies*
Albumin	P02768-1	FQNALLVR KVPQVSTPTLVEVSR	69,293	2	*Bos taurus*, *Ovis aries*
Collagen type III alpha 1 chain	G1PR85	GGPGPAGPR GPAGPQGPR GPVGPSGPPGK	139,958	3	*Bos taurus*
Collagen type I alpha 2 chain	G1PSJ6	GEAGAAGPAGPAGPR GVVGPQGAR VGAPGPAGAR	129,047	3	*Bos taurus*
Collagen type I alpha 1 chain	G1T4A5	DGEAGAQGPPGPAGPAGER GFSGLDGAK GVPGPPGAVGPAGK GVQGPPGPAGPR SAGVSVPGPMGPSGPR SGDRGETGPAGPAGPIGPAGAR	129,191	6	*Oryctolagus cunicilus*
Collagen type I alpha 2 chain	H0VHD0	GEAGPAGPAGPAGPR	123,053	1	*Cavia porcellus*
Ovalbumin	P01012	GGLEPINFQTAADQAR	42,881	1	*Gallus gallus*
Collagen type I alpha 1 chain	A0A8V1A970	GFSGLDGAK GPAGPQGPR	12,319	2	*Gallus gallus*

BLAST analysis (using the Swiss-Prot database, 2025 release, 574,627 reviewed entries) further validated the presence of ovalbumin in the samples by matching the identified peptide sequences.

In addition, several proteins were identified such as keratins, likely due to human contamination and other *Mammals* and *Gallus Gallus* proteins due to the presence of protein aggregated with binders on the paint (Supplementary Materials Table S1). High-resolution tandem MS allowed the characterization of several peptides and the identifications of proteins historically employed as binders in ancient paints [46,47]. The identification of

both animal skin (collagens) and egg white (ovalbumin) as binders suggests a complex and possibly layered painting technique, consistent with traditional polychrome practices. The presence of multiple protein materials may reflect different functional roles, such as ground preparation or pigment binding. The use of advanced mass spectrometry allows for sequencing a substantial portion of proteins with high identification accuracy, a level of detail that cannot be achieved with FTIR analysis. Moreover, this approach provides the significant advantage of determining the biological species from which the proteins originate (e.g., bovine, avian), a result that is not attainable through other analytical techniques, except for gene sequencing [18].

These results also reinforce the authenticity of the painting's materials because they confirm the use of known historical recipes and techniques used in polychrome artwork.

4. Conclusions

This study has demonstrated how an integrated analytical approach can effectively support both the conservation process and the technical investigation of Michele di Matteo's Coronation of the Virgin. In particular, colorimetric measurements acquired before and after the recent conservation intervention provided objective documentation of the effects of the surface cleaning, supported the evaluation of the appropriateness of the intervention outcome, and established a reference baseline for future monitoring of the conservation state of the artwork. In several areas, cleaning resulted in an increase in brightness and the recovery of chromatic tones closer to the original appearance, previously obscured by surface deposits. On the basis of these results, the cleaning outcome was considered satisfactory from a conservation point of view, supporting the decision not to proceed further with more invasive treatments.

Infrared reflectography played a key role in the examination of the underlying layers, revealing extensive portions of the preparatory drawings beneath the painted surface. These elements, including facial features and architectural lines, testify to the artist's careful planning of the composition. IRR also brought to light decorative punch marks and a crown above Christ's head that is no longer visible today, suggesting either changes in the original design or the effects of later alterations or losses.

The combined use of multispectral imaging, hyperspectral imaging and visible reflectance analysis allowed for the identification of several original pigments and the mapping of their distribution across the artwork, confirming and expanding upon the results of previous studies. Pigments such as cinnabar, azurite and green earth were identified as part of the original palette, while the presence of cadmium red on the cushion next to the Virgin was attributed to a later intervention.

In addition, the application of an advanced proteomic workflow demonstrated its effectiveness in the characterization of proteinaceous binding media, corroborating the historical use of animal-derived materials in paint binders.

Overall, the multi-method approach adopted in this work provided new and detailed insights into both the conservation history and the material composition of the painting. Rather than guiding the cleaning strategy itself, the analytical results contributed to the objective assessment of the intervention outcome and to informed conservation decision-making, as well as to the definition of reference data useful for future condition monitoring. The methodologies presented here may serve as a valuable reference for future investigations of complex polychrome artworks.

Supplementary Materials: The following supporting information can be downloaded at: https://www.mdpi.com/article/10.3390/heritage9020080/s1, Figure S1: Near-infrared fluorescence image under UV excitation highlighting localized retouching on the cushion; the Kremer reference chart including cadmium red is reported for comparison; Table S1: Identified proteins based on the Gallus

gallus UniProt database, with the number of peptides, molecular weight, accession numbers, and corresponding peptide sequences.

Author Contributions: Conceptualization, P.F. and V.C.; methodology, V.C., A.D. and P.F.; investigation, V.C., P.F., C.A.L., A.B., A.D., G.C., M.B., D.B., V.V., V.G. and M.C.; resources, P.F.; data curation V.C., C.A.L., M.B. and G.C.; validation, P.F., V.C. and A.D.; writing—Original Draft Preparation, V.C., P.F., C.A.L., A.B. and A.D.; review and editing V.C., P.F., A.B. and A.D.; Supervision, V.C. and P.F.; project administration, P.F.; funding acquisition, P.F. All authors have read and agreed to the published version of the manuscript.

Funding: Project funded by the European Union—NextGenerationEU, under the National Recovery and Resilience Plan (NRRP), Mission 4, Component 2, Investment Line 1.3, specifically within Spoke 6 (History, Conservation and Restoration of Cultural Heritage).

Data Availability Statement: The original contributions presented in this study are included in the article/Supplementary Materials. Further inquiries can be directed to the corresponding author.

Acknowledgments: The authors wish to thank Daniele Molina (Key Account Manager C&A, Konica Minolta Sensing Europe B.V., Italy Branch) for the technical and organizational support provided and for making the Specim INSIGHT software available on loan.

Conflicts of Interest: The authors declare no conflicts of interest.

References

1. Fermo, P.; Lombardi, C.A.; D'Amato, A.; Guglielmi, V.; Giudici, B.; Tomaino, A.; Pozzi, M.; Comite, V.; Bergomi, A.; Guardiano, L.; et al. Disclosing Colors and Pigments on Archaeological Objects from the Aga Khan Necropolis (West Aswan Egypt) through On-Site Analytical Methods: Preliminary Results. *Heritage* **2024**, *7*, 4980–4996. [CrossRef]
2. Fioretti, G.; Campobasso, C.; Eramo, G.; Monno, A.; Tempesta, G. On Devotional Artworks: A Non-Invasive Characterization of Pigments of the *Madonna della* Croce Wall Painting in Triggiano (Bari, Southern Italy). *Heritage* **2023**, *6*, 4263–4281. [CrossRef]
3. Klisinska-Kopacz, A.; Obarzanowski, M.; Fraczek, P.; Moskal-del Hoyo, M.; Gargano, M.; Goslar, T.; Chmielewski, F.; Dudała, J.; del Hoyo-Meléndez, M.J. An Analytical Investigation of a Wooden Panel Painting Attributed to the Workshop of Lucas Cranach the Elder. *J. Cult. Herit.* **2022**, *55*, 185–194. [CrossRef]
4. Volpi, F.; Fiocco, G.; Rovetta, T.; Invernizzi, C.; Albano, M.; Licchelli, M.; Malagodi, M. New Insights on the Stradivari 'Coristo' Mandolin: A Combined Non-Invasive Spectroscopic Approach. *Appl. Sci.* **2021**, *11*, 11626. [CrossRef]
5. Picollo, M.; Cucci, C.; Casini, A.; Stefani, L. Modern technologies for the study of painted artworks: From scanning imaging to the integrated use of non-invasive analytical techniques. *J. Cult. Herit.* **2020**, *45*, 258–269.
6. Dyer, J.; Sotiropoulou, S. A Technical Step Forward in the Integration of Visible-Induced Luminescence Imaging Methods for the Study of Ancient Polychromy. *Herit. Sci.* **2017**, *5*, 24. [CrossRef]
7. Cosentino, A. Practical Notes on Ultraviolet Technical Photography for Art Examination. *Conserv. Patrim.* **2015**, *21*, 53–62. [CrossRef]
8. Striova, J.; Salvadori, B.; Fontana, R.; Sansonetti, A.; Barucci, M.; Pampaloni, E.; Marconi, E.; Pezzati, L.; Colombini, M.P. Optical and spectroscopic tools for evaluating Er:YAG laser removal of shellac varnish. *Stud. Conserv.* **2015**, *60*, S91–S98. [CrossRef]
9. Lorusso, S.; Natali, A.; Matteucci, C. Colorimetry applied to the field of cultural heritage: Examples of study cases. *Conserv. Sci. Cult. Herit.* **2007**, *7*, 37–58. [CrossRef]
10. Cabello Briones, C.; Prendergast, H.; Stanley, C.; de la Torre, A.; Naemi, R.; Taylor, J.; McLaughlin, J. Colorimetry to assess the visual impact of dust deposition on mosaics at sheltered archaeological sites. *Herit. Sci.* **2021**, *9*, 40. [CrossRef]
11. Cesaratto, A.; Nevin, A.; Valentini, G.; Brambilla, L.; Castiglioni, C.; Toniolo, L.; Fratelli, M.; Comelli, D. A Novel Classification Method for Multispectral Imaging Combined with Portable Raman Spectroscopy for the Analysis of a Painting by Vincent Van Gogh. *Appl. Spectrosc.* **2013**, *67*, 1234–1241. [CrossRef]
12. Colantonio, C.; Clivet, L.; Laval, E.; Coquinot, Y.; Maury, C.; Melis, M.; Boust, C. Integration of Multispectral Imaging, XRF Mapping and Raman Analysis for Noninvasive Study of Illustrated Manuscripts: The Case Study of Fifteenth Century "Humay Meets the Princess Humayun" Persian Masterpiece from Louvre Museum. *Eur. Phys. J. Plus* **2021**, *136*, 958. [CrossRef]
13. Kogou, S.; Lucian, A.; Bellesia, S.; Bur-gio, L.; Bailey, K.; Brooks, C.; Liang, H. A Holistic Multimodal Approach to the Non-Invasive Analysis of Watercolour Paintings. *Appl. Phys. A* **2015**, *121*, 999–1014. [CrossRef]
14. Romano, C.; Dyer, J.; Shibayama, N. Reading Polychrome Laces: Multispectral Imaging Techniques on Historic Textiles from the Collections of The Metropolitan Museum of Art. *Dyes Hist. Archaeol.* **2021**, 33–34.

15. Bläuer, C.; Keller, A.T. Mainly Red and a Hidden Blue–Laboratory and MSI Investigations on the Carolingian Wall Paintings in the Chapel of the Holy Cross of Müstair (Switzerland). *J. Cult. Herit.* **2020**, *42*, 72–80. [CrossRef]
16. Leucci, G.; De Giorgi, L.; Masini, N. Towards an Integrated Approach to the Non-Invasive Diagnosis of Mural Paintings: The Case Study of Santa Maria della Croce (Apulia, Southern Italy). *J. Archaeol. Sci. Rep.* **2018**, *19*, 599–607.
17. Delledonne, C.; Albano, M.; Rovetta, T.; Borghi, G.; Gentile, M.; Marvelli, A.D.; Mezzabotta, P.; Riga, L.; Salvini, E.; Trucco, M.; et al. Rediscovering the Painting Technique of the 15th Century Panel Painting Depicting the Coronation of the Virgin by Michele di Matteo. *Heritage* **2024**, *7*, 324–337. [CrossRef]
18. Dallongeville, S.; Koperska, M.; Garnier, N.; Reille-Taillefert, G.; Rolando, C.; Tokarski, C. Identification of animal glue species in artworks using proteomics: Application to a 18th century gilt sample. *Anal. Chem.* **2011**, *83*, 9431–9437. [CrossRef] [PubMed]
19. Colombini, M.P.; Andreotti, A.; Bonaduce, I.; Modugno, F.; Ribechini, E. Analytical Strategies for Characterizing Organic Paint Media Using Gas Chromatography/Mass Spectrometry. *Acc. Chem. Res.* **2010**, *43*, 715–727. [CrossRef]
20. Andreotti, A.; Bonaduce, I.; Colombini, M.P.; Modugno, F.; Ribechini, E. Organic Paint Materials and Their Characterization by GC–MS Analytical Procedures. In *New Trends in Analytical, Environmental and Cultural Heritage Chemistry*; Tassi, L., Colombini, M.P., Eds.; Transworld Research Network: Kerala, India, 2008; pp. 389–423.
21. Mills, J.S.; White, R. *The Organic Chemistry of Museum Objects*, 2nd ed.; Butterworth-Heinemann: Oxford, UK, 1994.
22. van den Berg, J.D.J.; van den Berg, K.J.; Boon, J.J. Gas Chromatography/Mass Spectrometry of Diterpenoid Acids in Old Master Paintings. *J. Mass Spectrom.* **2000**, *35*, 512–533. [CrossRef]
23. van Keulen, H.; Boon, J.J. Analysis of Natural Organic Binding Media and Varnishes by Mass Spectrometric Techniques. *Stud. Conserv.* **1995**, *40*, 15–23.
24. Massaccesi, F. Nuove riflessioni sul percorso di Michele di Matteo. *Arte Cris.* **2009**, *97*, 171–180.
25. Amorini, A. *Le Vite dei Pittori ed Artefici Bolognesi*; Tipi Governativi alla Volpe: Bologna, Italy, 1841; Volume I.
26. Masini, C. *Bologna Perlustrata*; Stamperia di Longhi: Bologna, Italy, 1666.
27. Specim, a Konica Minolta Company. Available online: https://www.specim.com/products/speciminsight/ (accessed on 15 December 2025).
28. Burgio, L.; Clark, R.J.H. Library of FT-Raman spectra of pigments, minerals, pigment media and varnishes, and supplement to existing library of Raman spectra of pigments with visible excitation. *Spectrochim. Acta A Mol. Biomol. Spectrosc.* **2001**, *57*, 1491–1521. [CrossRef] [PubMed]
29. D'Amato, A.; Zilberstein, G.; Zilberstein, S.; Golovan, M.I.; Zhuravleva, A.A.; Righetti, P.G. Anton Chekhov and Robert Koch Cheek to Cheek: A Proteomic Study. *Proteomics* **2018**, *18*, e1700447. [CrossRef] [PubMed]
30. Kremer Pigmente. Available online: https://www.kremer-pigmente.com/en/shop/books-color-charts/color-charts/ (accessed on 14 August 2025).
31. Ciatti, M.; Frosinini, C. *La Tecnica Della Doratura e Della Punzonatura Nella Pittura Italiana del Medioevo e del Rinascimento*; Edifir: Firenze, Italy, 2002.
32. Anselmi, V. Michele di Matteo tra Bologna, Venezia e Siena—Alcune Nuove Proposte e un'Ipotesi di Riordino Cronologico. *Prospettiva* **2011**, *141*, 32–58.
33. Cosentino, A. FORS Spectral Database of Historical Pigments in Different Binders. *E-Conserv. J.* **2014**, *2*, 54–65. [CrossRef]
34. Guglielmi, V.; Lombardi, C.A.; Fiocco, G.; Comite, V.; Bergomi, A.; Borelli, M.; Azzarone, M.; Malagodi, M.; Colella, M.; Fermo, P. Multi-Analytical Investigation on a Renaissance Polychrome Earthenware Attributed to Giovanni Antonio Amadeo. *Appl. Sci.* **2023**, *13*, 3924. [CrossRef]
35. Vasco, G.; Aureli, H.; Fernández-Lizaranzu, I.; Moreno-Soto, J.; Križnar, A.; Parrilla-Giraldez, R.; Gómez-González, E.; Galisteo, M.A.R. Development of a Hyperspectral Imaging Protocol for Painting Applications at the University of Seville. *Heritage* **2024**, *7*, 5986–6007. [CrossRef]
36. Grissom, C.A. Green Earth. In *Artists' Pigments: A Handbook of Their History and Characteristics*; Archetype Publications: London, UK, 1986; Volume 1, pp. 141–168.
37. Casini, A.; Lotti, F.; Picollo, M.; Poggianti, L.; Stefani, L.; Buzzegoli, E. Fibre Optics Reflectance Spectroscopy and Hyper-Spectral Image Spectroscopy: Two Integrated Techniques for the Study of the Madonna dei Fusi. *Opt. Laser Eng.* **2000**, *34*, 291–299. [CrossRef]
38. Picollo, M.; Cucci, C.; Casini, A.; Stefani, L. Hyper-Spectral Imaging Technique in the Cultural Heritage Field: New Possible Scenarios. *Sensors* **2020**, *20*, 2843. [CrossRef]
39. Verni, E.; Albano, M.; Merlo, C.; Volpi, F.; Lee, C.; Lombardi, C.A.; Comite, V.; Fermo, P.; Bergomi, A.; Guglielmi, V.; et al. Non-Invasive Multi-Analytical Insights into Renaissance Wall Paintings by Bernardino Luini. *Coatings* **2025**, *15*, 1113. [CrossRef]
40. Knuutinen, U.; Mannerheimo, H.; Hornytzkyj, S. *Project Report of Pigment Analyses of the Fourth Style Wall Paintings in the Casa di Marco Lucrezio (IX 3, 5.24) in Pompeii*; EVTEK University of Applied Sciences: Helsinki, Finland, 2007.
41. Lyu, S.; Meng, D.; Hou, M.; Tian, S.; Huang, C.; Mao, J. Nonlinear Mixing Characteristics of Reflectance Spectra of Typical Mineral Pigments. *Minerals* **2021**, *11*, 626. [CrossRef]

42. Babini, A.; Green, P.; George, S.; Hardeberg, J.Y. Comparison of Hyperspectral Imaging and Fiber-Optic Reflectance Spectroscopy for Reflectance and Transmittance Measurements of Colored Glass. *Heritage* **2022**, *5*, 1401–1418. [CrossRef]
43. Agostino, A.; Pellizzi, E.; Aceto, M.; Castronovo, S.; Saroni, G.; Gulmini, M. On the Hierarchical Use of Colourants in a 15th Century Book of Hours. *Heritage* **2021**, *4*, 1786–1806. [CrossRef]
44. Coccato, C.; Moens, L.; Vandenabeele, P. On the stability of medieval inorganic pigments: Azurite degradation to green compounds such as malachite and basic copper chlorides. *Herit. Sci.* **2017**, *5*, 12. [CrossRef]
45. Ali, A.A.; Singh, M.R. From blue to green: A review of the use and alteration of azurite pigment in cultural heritage. *Arts Commun.* **2025**, *10*, 025220048. [CrossRef]
46. Dallongeville, S.; Garnier, N.; Rolando, C.; Tokarski, C. Proteomics for Cultural Heritage: Evaluation of Protein Extraction from Historic and Artistic Materials by In-Solution Digestion and Microwave-Assisted Digestion. *Anal. Chem.* **2011**, *83*, 9431–9437. [CrossRef]
47. Corso, G.; Gelzo, M.; Chambery, A.; Severino, V.; Di Maro, A.; Lomoriello, F.S.; D'Apolito, O.; Dello Russo, A.; Gargiulo, P.; Piccioli, C.; et al. Characterization of Pigments and Ligands in a Wall Painting Fragment from Liternum Archaeological Park (Italy). *J. Sep. Sci.* **2012**, *35*, 2986–2993. [CrossRef]